Maximal breaking of symmetry at critical angles and a closed-form expression for angular deviations of the Snell law

Manoel P. Araújo,[1] Silvânia A. Carvalho,[2] and Stefano De Leo[2,*]
[1]*Gleb Wataghin Physics Institute, State University of Campinas, Campinas, Brazil*
[2]*Department of Applied Mathematics, State University of Campinas, Campinas, Brazil*
(Received 3 July 2014; revised manuscript received 20 August 2014; published 25 September 2014)

A detailed analysis of the propagation of laser Gaussian beams at critical angles shows under which conditions it is possible to maximize the breaking of symmetry in the angular distribution and for which values of the laser wavelength and beam waist it is possible to find an analytic formula for the maximal angular deviation from the optical path predicted by the Snell law. For beam propagation through N dielectric blocks and for a maximal breaking of symmetry, a closed expression for the Goos-Hänchen shift is obtained. The multiple-peak phenomenon clearly represents additional evidence of the breaking of symmetry in the angular distribution of optical beams. Finally, the laser wavelength and beam-waist conditions to produce focal effects in the outgoing beam are also briefly discussed.

DOI: 10.1103/PhysRevA.90.033844 PACS number(s): 42.25.−p, 42.55.Ah

I. INTRODUCTION

It is well known that the Fresnel coefficients, which describe the propagation of optical beams between media with different refractive indexes, are useful in studying deviations from geometrical optics [1,2]. The most important examples are represented by the Goos-Hänchen [3–14] and Imbert-Fedorov [15–20] effects. For total internal reflection, Fresnel coefficients gain an additional phase, and this phase is responsible for the transversal shift of linearly and elliptically polarized light with respect to the optical beam path predicted by the Snell law. Nevertheless, these effects do *not* modify the angular predictions of geometrical optics. For example, for a dielectric block with parallel sides the outgoing beam is expected to be parallel to the incoming one. Angular deviations [21–25] from the optical path predicted by the Snell law are a direct consequence of the breaking of symmetry [26] in the angular distribution. In this paper, we show how to maximize this breaking of symmetry and give an *analytic formula* for the Snell law angular deviations. Two interesting additional phenomena, i.e., multiple peaks and the focal effect, appear in the analysis of the outgoing beam. In view of possible experimental investigations, our study, done for $n = \sqrt{2}$ for simplicity of presentation, is then extended to Borosilicate (BK7) or fused silica dielectric blocks and He-Ne lasers with $\lambda = 633\,\text{nm}$ and beam waists $w_0 = 100\,\mu\text{m}$ and 1 mm.

II. ASYMMETRICALLY MODELED BEAMS

As anticipated in the Introduction, the breaking of symmetry [26] in the angular distribution of optical beams plays a fundamental role in the angular deviation from the optical path predicted by the Snell law. In this section, to understand why the breaking of symmetry is responsible for such a fascinating phenomenon, we briefly discuss a maximal breaking of symmetry for an asymmetrically modeled beam. The effect of this maximal breaking of symmetry on the peak and the position mean value of the optical beam sheds light on the possibility to realize an optical experiment.

First of all, let us consider the *symmetric* Gaussian angular distribution

$$g(\theta) = \exp[-(k\, w_0\, \theta)^2/4], \tag{1}$$

where w_0 is the beam waist of the Gaussian laser and $k = 2\pi/\lambda$ is the wave number associated with the wavelength λ. The optical beam, propagating in the y-z plane, is represented by [19,20]

$$E(y,z) = E_0\, \frac{k\, w_0}{2\sqrt{\pi}} \int d\theta\; g(\theta)\, \exp[ik(\sin\theta y + \cos\theta z)]. \tag{2}$$

For $kw_0 \gg 1$, we can develop the sine and cosine functions up to the second order in θ. The electric field,

$$E(y,z) = \frac{E_0}{\gamma(z)} \exp\left\{ikz - \left[\frac{y}{w_0\gamma(z)}\right]^2\right\} = E_0 e^{ikz}\mathcal{G}(y,z), \tag{3}$$

where $\gamma(z) = \sqrt{1 + 2iz/kw_0^2}$, thus propagates along the z direction and manifests a cylindrical symmetry about the direction of propagation. The complex Gaussian function $\mathcal{G}(y,z)$ is the solution of the paraxial Helmholtz equation [1,2]

$$(\partial_{yy} + 2ik\partial_z)\mathcal{G}(y,z) = 0. \tag{4}$$

The optical intensity,

$$I(y,z) = |E(y,z)|^2 = \frac{I_0}{|\gamma(z)|^2} \exp\left[-\frac{2y^2}{w_0^2|\gamma(z)|^4}\right] = I_0 \frac{w_0}{w(z)} \exp\left[-\frac{2y^2}{w^2(z)}\right], \tag{5}$$

is a function of the axial (z) and transversal (y) coordinates. The Gaussian function $|\mathcal{G}(y,z)|$ has its peak on the z axis at $y = 0$, and its beam width increases with the axial distance z, as illustrated in Fig. 1(a). Because the Gaussian distribution $g(\theta)$ is a symmetric distribution centered at $\theta = 0$,

$$\langle y\rangle_{|\mathcal{G}|} = \frac{\int dy\, y|E(y,z)|^2}{\int dy|E(y,z)|^2} = \frac{\int dy\, y|\mathcal{G}(y,z)|^2}{\int dy|\mathcal{G}(y,z)|^2} = 0. \tag{6}$$

*deleo@ime.unicamp.br

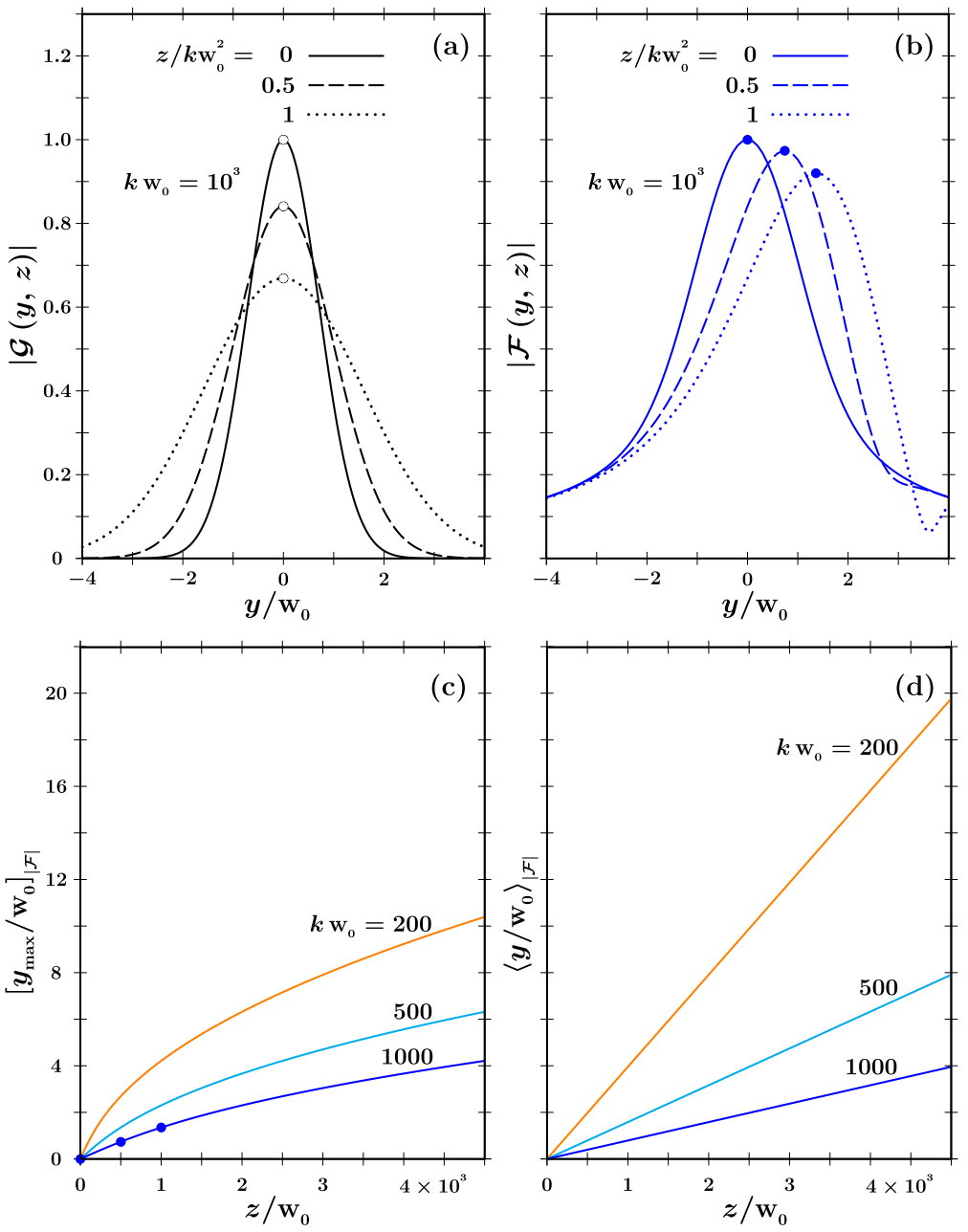

FIG. 1. (Color online) (a) Modeled breaking of symmetry. (b) The breaking of symmetry in the Gaussian angular distribution generates an axial dependence for the peak of the optical beam. This dependence is shown in (c). For the transversal mean value it is possible to obtain an axial linear analytical expression, given in Eq. (10), which is confirmed by the numerical data plotted in (d).

The previous analytical result shows that for symmetric distributions the peak position and transversal mean value coincide and do *not* depend on the axial parameter z. The symmetry in the angular distribution $g(\theta)$ is thus responsible for the well-known stationary behavior of the Gaussian laser peak.

To see how the breaking of symmetry drastically changes the previous situation, we model a *maximal* breaking of symmetry by considering the following *asymmetric* angular distribution:

$$f(\theta) = \begin{cases} 0 & \theta < 0, \\ \exp[-(kw_0\theta)^2/4] & \theta \geqslant 0. \end{cases} \tag{7}$$

This distribution determines the behavior of the new electric field,

$$\mathcal{E}(y,z) = \mathcal{E}_0\{1 + \mathrm{erf}[iy/w_0\gamma(z)]\}\mathcal{G}(y,z) = \mathcal{E}_0 e^{ikz}\mathcal{F}(y,z). \tag{8}$$

The asymmetry in the angular distribution of Eq. (7) is responsible for the axial dependence of the peak position [see Fig. 1(b)]. This z dependence is caused by the interference between the Gaussian and the error function which now appears in Eq. (8). The numerical analysis, done for different values of kw_0 and illustrated in Figs. 1(c) and 1(d), shows a different behavior between the peak position and transversal

mean value and confirms the analytical expression

$$\langle y\rangle_{|\mathcal{F}|} = \frac{\int dy\, y|\mathcal{F}(y,z)|^2}{\int dy|\mathcal{F}(y,z)|^2} = \frac{-\frac{i}{2k}\int d\theta f(\theta)e^{-ik\theta^2 z/2}\frac{\partial}{\partial\theta}[f(\theta)e^{-ik\theta^2 z/2}]^*}{\int d\theta f^2(\theta)} + \text{H.c.} = \frac{\int d\theta\theta f^2(\theta)}{\int d\theta f^2(\theta)}z = \frac{\sqrt{2/\pi}}{kw_0}z. \quad (9)$$

Finally, the breaking of symmetry in the modeled angular distribution, Eq. (7), generates deviations from the optical path, $y = 0$, expected by geometrical optics. The modeled beam now shows the angular deviation

$$\alpha_{\max} = \arctan\left[\frac{\sqrt{2/\pi}}{kw_0}\right], \quad (10)$$

where the subscript index has been introduced to recall that this angular deviation is due to the *maximal* breaking of symmetry introduced to model the Gaussian optical beam. This deviation can be physically understood by observing that for a symmetric distribution [see $g(\theta)$ in Eq. (1)], negative and positive angles play the same role, and consequently, their final contribution does not change the propagation of the optical path whose maximum is always centered at $y = 0$. In the case of the asymmetric distribution $f(\theta)$ given in Eq. (7) only positive angles contribute to the motion, and this generates a *maximal* angular deviation which clearly depends on the parameter kw_0. In the plane-wave limit, this deviation tends to zero.

The results presented in this section stimulate us to investigate in which situations Gaussian lasers, propagating through dielectric blocks, could experience a breaking of symmetry in their angular distributions similar to the modeled breaking of symmetry analyzed in this section. If this happens, the angular deviation from the optical path predicted by the Snell law should be equal to the angle α given in Eq. (10).

III. PROPOSING THE BREAKING OF SYMMETRY IN OPTICAL EXPERIMENTS

In this section, we treat the general problem of the transmission of a Gaussian optical beam through a dielectric block and study how to realize the breaking of symmetry which allows us to reproduce the effects discussed in the previous section. This section contains only a *proposal* to observe the breaking of symmetry in real optical experiments and to see under what circumstances it is possible to reproduce the maximal angular deviation $\alpha_{\max}$ of Eq. (10). In this proposal, we do not take into account cumulative dissipation effects. Imperfections such as misalignment of the dielectric surfaces will be discussed in the final section.

The optical beam represented by the electric field of Eq. (2) moves from its source S to the left interface of the dielectric block along the z axis [see Fig. 2(a)]. The $\tilde{z}$ and z_* directions represent, respectively, the left and right and up and down stratifications of the dielectric block. By observing that

$$\begin{pmatrix} y \\ z \end{pmatrix} = \begin{pmatrix} \cos\theta_0 & -\sin\theta_0 \\ \sin\theta_0 & \cos\theta_0 \end{pmatrix}\begin{pmatrix} \tilde{y} \\ \tilde{z} \end{pmatrix}, \quad (11)$$

we can immediately rewrite the incoming electric field in terms of the new axes $\tilde{y}$ and $\tilde{z}$,

$$E_{\text{inc}}(y,z) = E_0\frac{kw_0}{2\sqrt{\pi}}\int d\theta g(\theta)\exp[ik(\sin\theta y + \cos\theta z)] = E_0\frac{kw_0}{2\sqrt{\pi}}\int d\theta g(\theta)\exp\{ik[\sin(\theta+\theta_0)\tilde{y} + \cos(\theta+\theta_0)\tilde{z}]\} = E_0\frac{kw_0}{2\sqrt{\pi}}\int d\theta g(\theta-\theta_0)\exp[ik(\sin\theta\tilde{y} + \cos\theta\tilde{z})]. \quad (12)$$

At the first (left) and last (right) interfaces, $\sin\theta = n\sin\psi$ (see the dielectric block of Fig. 2). In terms of these angles, the transmission Fresnel coefficients for s-polarized waves are

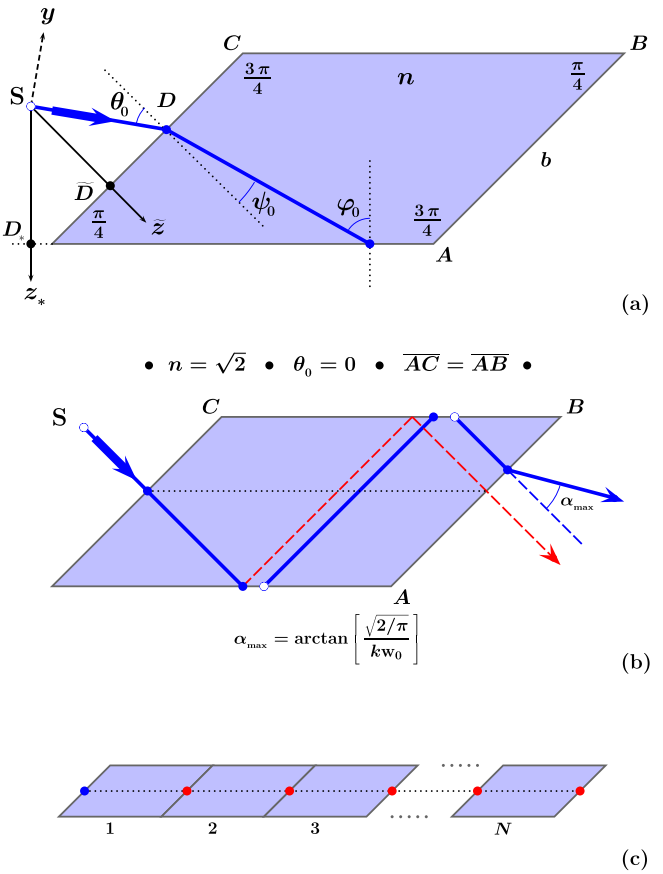

FIG. 2. (Color online) Geometry of the dielectric block. The normals of the left and right and up and down interfaces and the angular parameters which appear in the transmission coefficient are given in (a). For a symmetric angular distribution the outgoing beam is parallel to the incoming one. The breaking of symmetry generates an angular deviation α of the Snell law, which is drawn in (b) together with the transversal Goos-Hänchen shift. The breaking of symmetry is maximized by building a dielectric structure of N blocks in (c) which in a real optical experiment can be realized by a single elongated prism with sides $N\overline{BC}$ and $\overline{AB}$.

given by [1,2]

$$\{T^{[s]}_{\rm left}, T^{[s]}_{\rm right}\} = \left\{ \frac{2\cos\theta}{\cos\theta + n\cos\psi} e^{i\phi_{\rm left}}, \frac{2n\cos\psi e^{i\phi_{\rm right}}}{\cos\theta + n\cos\psi} e^{i\phi_{\rm right}} \right\}, \tag{13}$$

where

$$\phi_{\rm left} = k(\cos\theta - n\cos\psi)\overline{S\widetilde{D}},$$

$$\phi_{\rm right} = k(n\cos\psi - \cos\theta)\left(\overline{S\widetilde{D}} + \frac{\overline{BC}}{\sqrt{2}}\right).$$

The phase which appears in the Fresnel coefficients contains information on the point at which the beam encounters the air-dielectric (dielectric-air) interface, and it is obviously equal for s- and p-polarized waves [27–29]. At the second (down) and third (up) interfaces, observing that $\varphi = \psi + \frac{\pi}{4}$ [see Fig. 2(a)], the reflection Fresnel coefficients read

$$\{R^{[s]}_{\rm down}, R^{[s]}_{\rm up}\} = \frac{n\cos\varphi - \sqrt{1 - n^2\sin^2\varphi}}{n\cos\varphi + \sqrt{1 - n^2\sin^2\varphi}} \{e^{i\phi_{\rm down}}, e^{i\phi_{\rm up}}\}, \tag{14}$$

where

$$\phi_{\rm down} = 2kn\cos\varphi\overline{SD_*} \quad \text{and} \quad \phi_{\rm up} = 2kn\cos\varphi\left(\frac{\overline{AB}}{\sqrt{2}} - \overline{SD_*}\right).$$

The total transmission coefficient for s-polarized waves which propagate through the dielectric block sketched in Fig. 2(a) is then obtained by multiplying the Fresnel coefficients given in Eqs. (13) and (14),

$$T^{[s]}(\theta) = \frac{4n\cos\psi\cos\theta}{(\cos\theta + n\cos\psi)^2} \times \left(\frac{n\cos\varphi - \sqrt{1 - n^2\sin^2\varphi}}{n\cos\varphi + \sqrt{1 - n^2\sin^2\varphi}}\right)^2 e^{i\Phi_{\rm Snell}}, \tag{15}$$

where

$$\Phi_{\rm Snell} = k\left[\sqrt{2}n\cos\varphi\overline{AB} + (n\cos\psi - \cos\theta)\frac{\overline{BC}}{\sqrt{2}}\right].$$

In a similar way, we can immediately obtain the transmission coefficient for p-polarized waves [28,29],

$$T^{[p]}(\theta) = \frac{4n\cos\psi\cos\theta}{(n\cos\theta + \cos\psi)^2} \times \left(\frac{\cos\varphi - n\sqrt{1 - n^2\sin^2\varphi}}{\cos\varphi + n\sqrt{1 - n^2\sin^2\varphi}}\right)^2 e^{i\Phi_{\rm Snell}}. \tag{16}$$

Before we discuss the effect of the transmission coefficient on the angular Gaussian distribution, $g(\theta - \theta_0)$, let us spend some time analyzing the phase $\Phi_{\rm Snell}$ which appears in the transmission coefficient. The stationary phase approximation [30–32], which is a basic principle of asymptotic analysis based on the cancellation of sinusoids with a rapidly varying phase, allows us to obtain a prediction of the beam peak position by imposing

$$\left[\frac{\partial}{\partial\theta}(k\sin\theta\widetilde{y}_{\rm out} + k\cos\theta\widetilde{z}_{\rm out} + \Phi_{\rm Snell})\right]_{\theta=\theta_0} = 0.$$

This stationary constraint implies

$$\begin{aligned}\cos\theta_0\widetilde{y}_{\rm out} - \sin\theta_0\widetilde{z}_{\rm out} &= \sqrt{2}\sin\varphi_0\frac{\cos\theta_0}{\cos\psi_0}\overline{AB} + \left(\sin\psi_0\frac{\cos\theta_0}{\cos\psi_0} - \sin\theta_0\right)\frac{\overline{BC}}{\sqrt{2}} \\ &= \underbrace{\cos\theta_0\left[(1+\tan\psi_0)\overline{AB} + (\tan\psi_0 - \tan\theta_0)\frac{\overline{BC}}{\sqrt{2}}\right]}_{d_{\rm Snell}}. \end{aligned} \tag{17}$$

This reproduces the well-known transversal shift obtained in geometrical optics by using the Snell law. With respect to the incoming optical beam, which is centered at $y = 0$, the center of the outgoing beam is then shifted at $y = d_{\rm Snell}$. To ensure that for the dielectric structure illustrated in Fig. 2(c) we have $2N$ internal reflections, we must impose the condition that, in each block, incoming and outgoing beams have the same z_* component; this implies

$$\overline{BC} = \sqrt{2}\tan\varphi_0\overline{AB}. \tag{18}$$

In this case, the propagation of the optical beam through N dielectric blocks is characterized by $2N$ internal reflections. For an elongated prism with a side $N\overline{BC}$, the transmission coefficients for s- and p-polarized waves are then given by

$$T^{[s]}_N(\theta) = \frac{4n\cos\psi\cos\theta}{(\cos\theta + n\cos\psi)^2} \times \left(\frac{n\cos\varphi - \sqrt{1 - n^2\sin^2\varphi}}{n\cos\varphi + \sqrt{1 - n^2\sin^2\varphi}}\right)^{2N} e^{iN\Phi_{\rm Snell}} \tag{19}$$

and

$$T^{[p]}_N(\theta) = \frac{4n\cos\psi\cos\theta}{(n\cos\theta + \cos\psi)^2} \times \left(\frac{\cos\varphi - n\sqrt{1 - n^2\sin^2\varphi}}{\cos\varphi + n\sqrt{1 - n^2\sin^2\varphi}}\right)^{2N} e^{iN\Phi_{\rm Snell}}. \tag{20}$$

For incidence angles less than the critical angle,

$$\theta < \theta_c = \arcsin\left\{n\sin\left[\arcsin\left(\frac{1}{n}\right) - \frac{\pi}{4}\right]\right\},$$

the outgoing optical beam,

$$\begin{aligned} E^{[s,p]}_T(y,z) &= E_0\frac{kw_0}{2\sqrt{\pi}}\int d\theta T^{[s,p]}_N(\theta)g(\theta - \theta_0) \\ &\quad \times \exp[ik(\sin\theta\widetilde{y} + \cos\theta\widetilde{z})] \\ &= E_0\frac{kw_0}{2\sqrt{\pi}}\int d\theta g^{[s,p]}_T(\theta;\theta_0) \\ &\quad \times \exp\{ik[\sin(\theta - \theta_0)y + \cos(\theta - \theta_0)z]\}, \end{aligned} \tag{21}$$

propagates parallel to the z axis, with its peak located at

$$y_{\rm Snell} = Nd_{\rm Snell} = N(\cos\theta_0 - \sin\theta_0)\tan\varphi_0\overline{AB}, \tag{22}$$

as expected from the ray optics. For incidence angles greater than the critical angle, we find $\sin\varphi > 1$ and the optical beam gains an *additional* phase,

$$N\Phi^{[s,p]}_{\rm GH}, \tag{23}$$

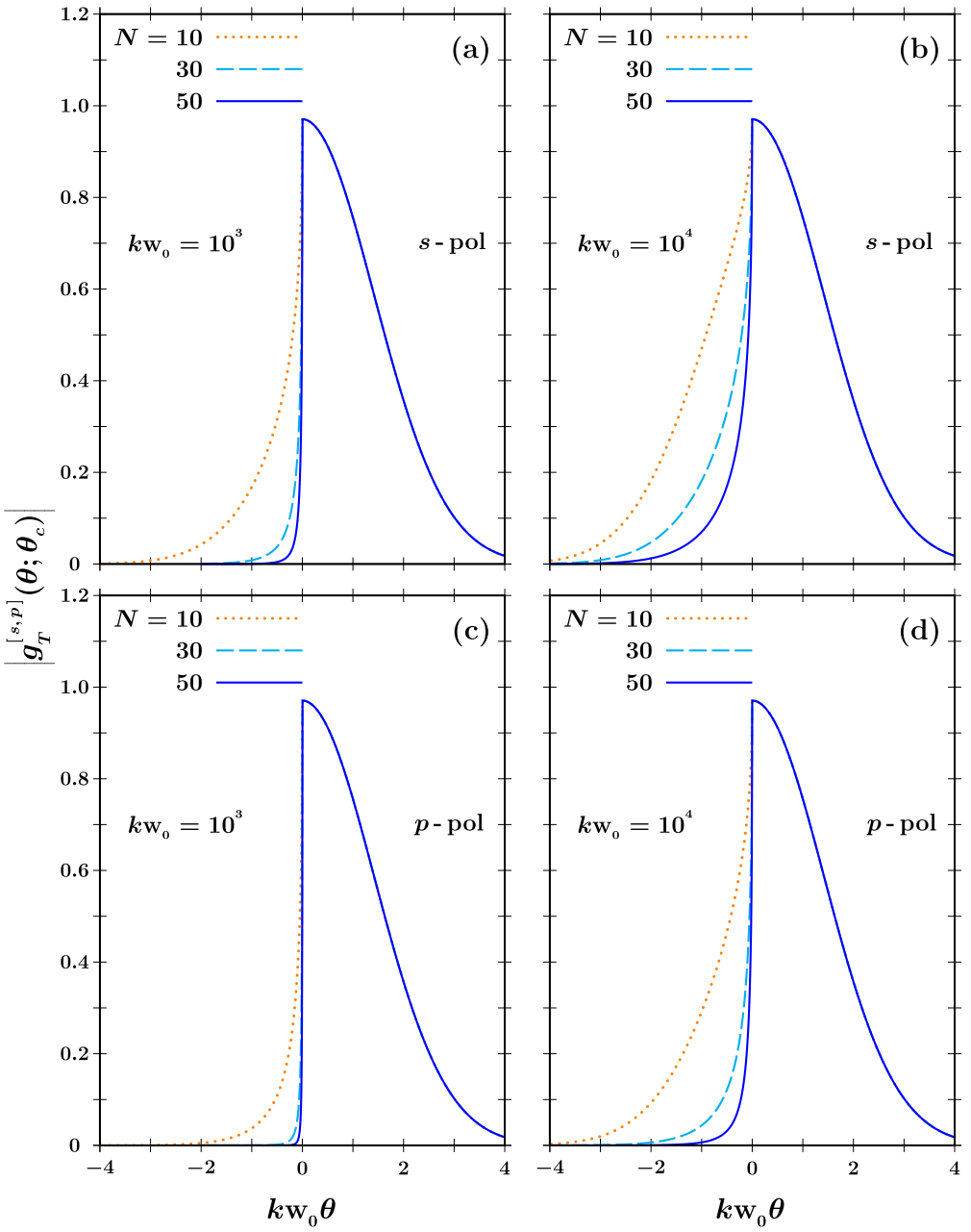

FIG. 3. (Color online) Symmetry breaking for N dielectric blocks. The modeled breaking of symmetry discussed in Sec. II is now proposed for optical experiments at critical incidence ($\theta_c = 0, \varphi_c = \pi/4$). The plots show that to maximize the breaking of symmetry, we have to decrease the beam waist, increase the blocks number, and use p-polarized waves. For p-polarized waves, an optimal choice to obtain a *maximal* breaking of symmetry is represented by $N = 50$ and $kw_0 = 10^3$. To reproduce the maximal symmetry breaking for the other cases, we have to increase the number of blocks.

where

$$\Phi_{\mathrm{GH}}^{[s,p]} = \begin{cases} -4 \arctan \sqrt{(n^2 \sin^2 \varphi - 1)/(n \cos \varphi)^2} & (s \text{ polarization}], \\ -4 \arctan \sqrt{n^2 (n^2 \sin^2 \varphi - 1)/ \cos^2 \varphi} & (p \text{ polarization}). \end{cases} \tag{24}$$

For linearly polarized light, this new phase is responsible for the Goos-Hänchen shift. This shift was experimentally observed in 1947 [3], and one year later, Artmann [4] proposed an analytical expression. The Artmann formulas, valid for an incidence angle greater than the critical angle, have recently been generalized for incidence at the critical angle [14]. Notwithstanding the interesting nuances involved in the study of the Goos-Hänchen shift, what we aim to discuss in detail in this paper is the *angular deviation* from the optical path predicted by the Snell law.

The angular deviation $\alpha_{\max}$, given in Eq. (10), is due to the *maximal* breaking of symmetry modeled in Sec. II [see Eq. (7)]. In the dielectric structure illustrated in Fig. 2(c) (observe that in a real optical experiment this structure can be reproduced by a single elongated prism with a side $N\overline{BC}$), the optical beam experiences $2N$ internal reflections, and this will play a fundamental role in reproducing, for incidence at the critical angle, the maximal breaking of symmetry presented in Sec. II using a modeled example. Indeed, for incidence at the critical angle, the angular distribution $g_T^{[s,p]}(\theta;\theta_c)$ centered at $\theta = \theta_c$ experiences, at each up and down interface, a partial transmission for $\theta < \theta_c$ and a total reflection for $\theta > \theta_c$. Consequently, by increasing the number of internal reflections we contribute to the increase in the breaking of symmetry. For a few blocks, the real optical experiment is very different from the modeled case presented in Sec. II. Nevertheless, for $N \gg 1$, we improve the breaking of symmetry and can simulate the maximal breaking of symmetry discussed in Sec. II. From Fig. 3, where we plot the modulus of the transmitted angular distribution $g_T^{[s,p]}(\theta;\theta_c)$, we can immediately see that the breaking of symmetry is optimized not only by increasing the number of blocks but also by using p-polarized waves and/or decreasing the value of the beam waist. As shown in Fig. 3(c), for $kw_0 = 10^3$ (which for a He-Ne laser with

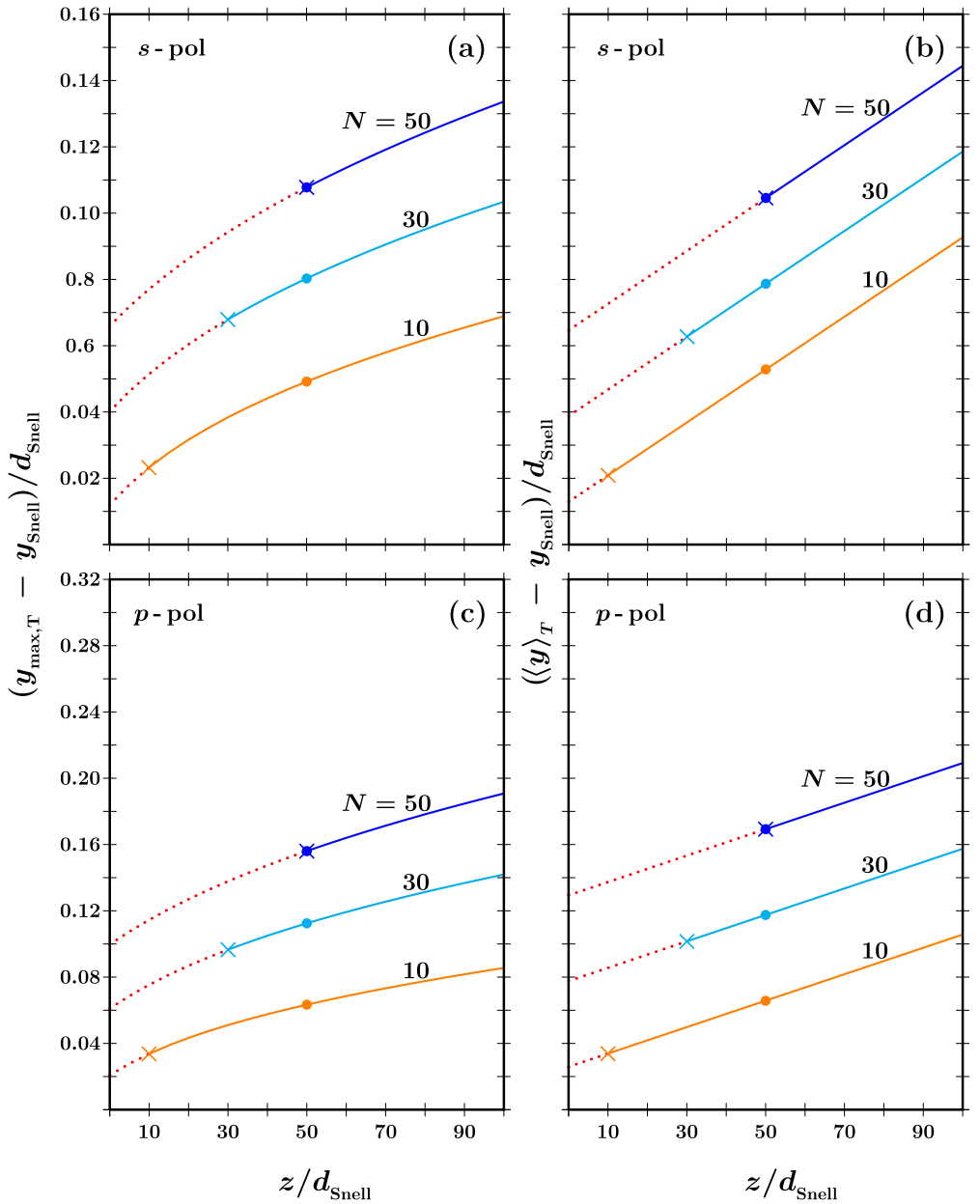

FIG. 4. (Color online) Snell's law angular deviation. The axial dependence at the critical angle $\theta_c = 0$ of the peak and transversal mean value are plotted for a fixed beam waist w_0, $kw_0 = 10^3$, and $b/w_0 = 10^2$ for different block numbers N. The angular deviation of the Snell law is evident in (b) and (d). Observe that the first physical axial points at which we can perform the experimental analysis are given by $z_{\text{out}} = z_{\text{in}} + N \tan\varphi_c \overline{AB}$ (crosses in the plots). From the plots the N amplification of the Goos-Hänchen shift at the critical angle is also clear. The circles represent the points at which the numerical calculation has also been done for BK7 and fused silica blocks (Table I).

TABLE I. (Color online) Snell's law angular deviation for BK7 and fused silica dielectric blocks. Numerical peak position $y_{\max,T}$ and transversal mean value $\langle y\rangle_T$ of the transmitted beam at the critical angle $\theta_0=\theta_c$ are listed for s- and p-polarized waves for different refractive indexes as a function of the number of blocks N and for fixed beam waist/wavelength ratio, $kw_0=10^3$, and axial parameter, $z=50d_{\text{Snell}}$. We immediately see that by increasing the number of blocks (and consequently optimizing the breaking of symmetry) we increase the angular deviation of the Snell law.

	$y_{\max}/d_{\text{Snell}}-N$			$\langle y/d_{\text{Snell}}\rangle-N$			
n \ N	10	30	50	10	30	50	
$\sqrt{2}$	0.050	0.080	0.108	0.053	0.079	0.104	s-pol
1.457	0.049	0.079	0.105	0.052	0.077	0.102	s-pol
1.515	0.047	0.077	0.102	0.051	0.075	0.099	s-pol
$\sqrt{2}$	0.063	0.112	0.156	0.066	0.117	0.170	p-pol
1.457	0.064	0.113	0.158	0.066	0.119	0.171	p-pol
1.515	0.064	0.114	0.159	0.067	0.120	0.174	p-pol

$\lambda=633$ nm means $w_0\approx 100\,\mu$m), $N=50$, and p-polarized waves, we *perfectly* reproduce the modeled breaking of symmetry illustrated in Sec. II. By increasing the number of blocks or, equivalently, the side of the elongated prism, we can always reach the maximal breaking of symmetry (7). It is important to note here that such a distribution leads to the *maximal* angular deviation. For incidence not at the critical angle or in the presence of misalignment at the dielectric surfaces, the angular deviation decreases (see the discussion at the end of Sec. V).

IV. SNELL LAW ANGULAR DEVIATION, MULTIPLE-PEAK PHENOMENON, AND FOCAL EFFECT

As observed in the previous section, it is possible to reproduce in a real optical experiment the modeled breaking of symmetry introduced in Sec. II. The preferred incidence angle is $\theta_0=\theta_c$. In this case, for an appropriate choice of the number of dielectric blocks ($N=50$) and of the laser beam waist ($kw_0=10^3$), it is possible to take the following approximation:

$$g_T^{[s,p]}(\theta;\theta_c)=\left|g_T^{[s,p]}(\theta;\theta_c)\right|e^{iN(\Phi_{\text{Snell}}+\Phi_{\text{GH}}^{[s,p]})}\approx f(\theta-\theta_c)e^{iN(\Phi_{\text{Snell}}+\Phi_{\text{GH}}^{[s,p]})}. \tag{25}$$

The transversal mean value for the outgoing beam is then given by

$$\begin{aligned}\langle y\rangle_{T,c}^{[s,p]}&=\frac{-\frac{i}{2k}\int d\theta g_T^{[s,p]}(\theta;\theta_c)e^{-ik(\theta-\theta_c)^2z/2}\frac{\partial}{\partial\theta}\left[g_T^{[s,p]}(\theta;\theta_c)e^{-ik(\theta-\theta_c)^2z/2}\right]^*}{\int d\theta\left|g_T^{[s,p]}(\theta;\theta_c)\right|^2}+\text{H.c.}\\&=\frac{\int d\theta\left[-\frac{N}{k}\frac{\partial}{\partial\theta}\left(\Phi_{\text{Snell}}+\Phi_{\text{GH}}^{[s,p]}\right)+(\theta-\theta_c)z\right]f^2(\theta-\theta_c)}{\int d\theta f^2(\theta-\theta_c)}\\&=y_{\text{Snell},c}+y_{\text{GH},c}^{[s,p]}+\frac{\sqrt{2/\pi}}{kw_0}z.\end{aligned} \tag{26}$$

The Snell law angular deviation α [see Eq. (10) and Fig. 2(b)] obtained in Sec. II for a modeled breaking of symmetry can now be reproduced in a real optical experiment. For a partial breaking of symmetry the angular deviation is obviously reduced, and a numerical calculation is needed to estimate such a deviation (see Fig. 4). The peak position and the transversal component mean value, plotted in Fig. 4 for $n=\sqrt{2}$, which has been chosen because a dielectric block with such a refractive index has a critical angle $\theta_c=0$ ($\varphi_c=\pi/4$), have also been calculated for dielectric fused silica ($n=1.457$) and BK7 ($n=1.515$) blocks,

$$\left\{n,\frac{180^\circ\theta_c}{\pi},\frac{180^\circ\varphi_c}{\pi}\right\}=\{\sqrt{2},0^\circ,45^\circ\},\quad\{1.457,-2.42^\circ,43.34^\circ\},\quad\{1.515,-5.60^\circ,41.31^\circ\}$$

(see Table I). It is important to observe that by increasing the number of blocks we reach the maximal breaking of symmetry. In the Snell and Goos-Hänchen shifts, we find a *linear* dependence on the block number,

$$y_{\text{Snell},c}=N(\cos\theta_c-\sin\theta_c)\tan\varphi_c\overline{AB}=N\frac{\sqrt{2-n^2+2\sqrt{n^2-1}}-1+\sqrt{n^2-1}}{\sqrt{2(n^2-1)}}\overline{AB}=N\delta_{\text{Snell},c}\overline{AB} \tag{27}$$

and

$$\begin{aligned}\{y_{\text{GH},c}^{[s]},y_{\text{GH},c}^{[p]}\}&=N\{1,n^2\}\frac{\frac{4}{k}\int d\theta\sqrt{\frac{\cos\theta_c}{n\cos\psi_c(n^2-2\sin^2\theta_c)(\theta-\theta_c)}}f^2(\theta-\theta_c)}{\int d\theta f^2(\theta-\theta_c)}\\&=N\{1,n^2\}\frac{4\Gamma(1/4)}{\sqrt{\pi\sqrt{2}}}\left[\frac{2-n^2+2\sqrt{n^2-1}}{4(n^2-1)(n^2+2\sqrt{n^2-1})}\right]^{1/4}\sqrt{\frac{w_0}{k}}=N\{1,n^2\}\delta_{\text{GH},c}\sqrt{\frac{w_0}{k}}.\end{aligned} \tag{28}$$

Note that the divergence at the critical angle is removed by the previous integration. Consequently, for a maximal breaking of symmetry, we find an analytical expression for the Goos-Hänchen shift at the critical angle. Observing that

$$\{n,\delta_{\text{Snell},c},\delta_{\text{GH},c}\}=\{\sqrt{2},1,4.091\},\quad\{1.457,0.983,3.915\},\quad\{1.515,0.960,3.700\},$$

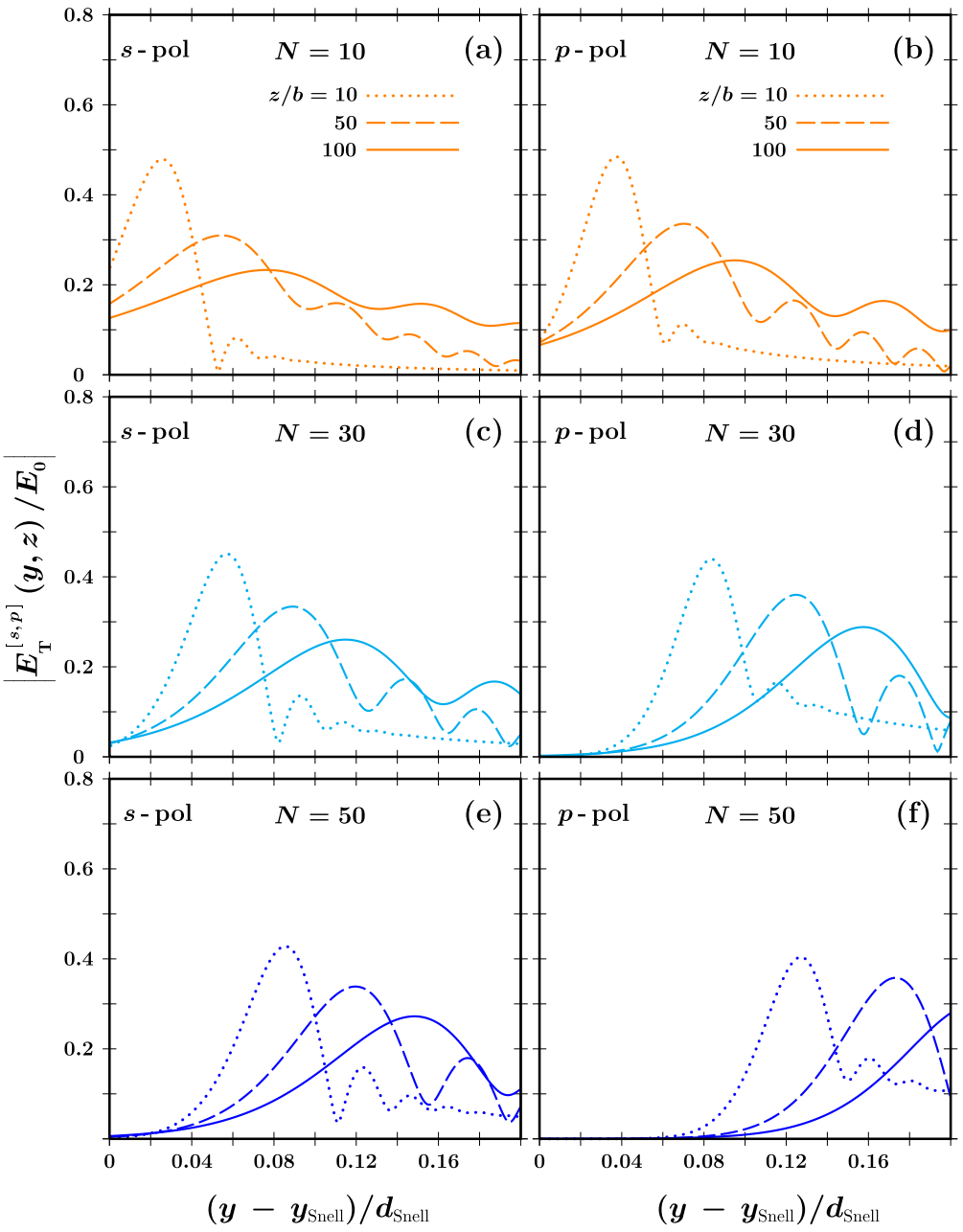

FIG. 5. (Color online) Multiple-peak phenomenon. For $kw_0 = 10^3$, $b/w_0 = 10^2$ and for incidence at the critical angle, the outgoing optical beam presents the fascinating phenomenon of multiple peaks. This phenomenon is directly related to the spreading of the optical beam, and it occurs because in the angular distribution the positive angular components are no longer compensated by the negative ones.

in the N-block dielectric structure of Fig. 2(c), we have a Snell shift proportional to $N\overline{AB}$ and an amplification of the standard Goos-Hänchen shift ($\sim\lambda$) given by $N\sqrt{kw_0}$. The numerical analysis done in Fig. 4 and Table I confirms this amplification.

The multiple-peak phenomenon observed in Fig. 5 is clear evidence of the breaking of symmetry in the angular distribution. In the optical beam, the negative angular contributions are suppressed if we increase the number of blocks. This implies that there are only positive angular contributions in the spreading of the optical beam and, consequently, the multiple-peak phenomenon. As can be seen in Fig. 5, this phenomenon is amplified not only by increasing the number of blocks but also by using p-polarized waves. Note that the phenomenon is more evident when the spreading of the optical beam is clearly visible. Figure 6 presents another interesting phenomenon. The focal effect in the outgoing beam is a consequence of the second-order contribution of the optical phase which is responsible for the spreading of the beam. The numerical analysis [see Fig. 6(f) and Table II] shows an increasing value of the maximum of the outgoing electrical field, and this is clear evidence of a focalization of the beam. From the data presented in Table II, we can estimate the axial point of maximal focalization.

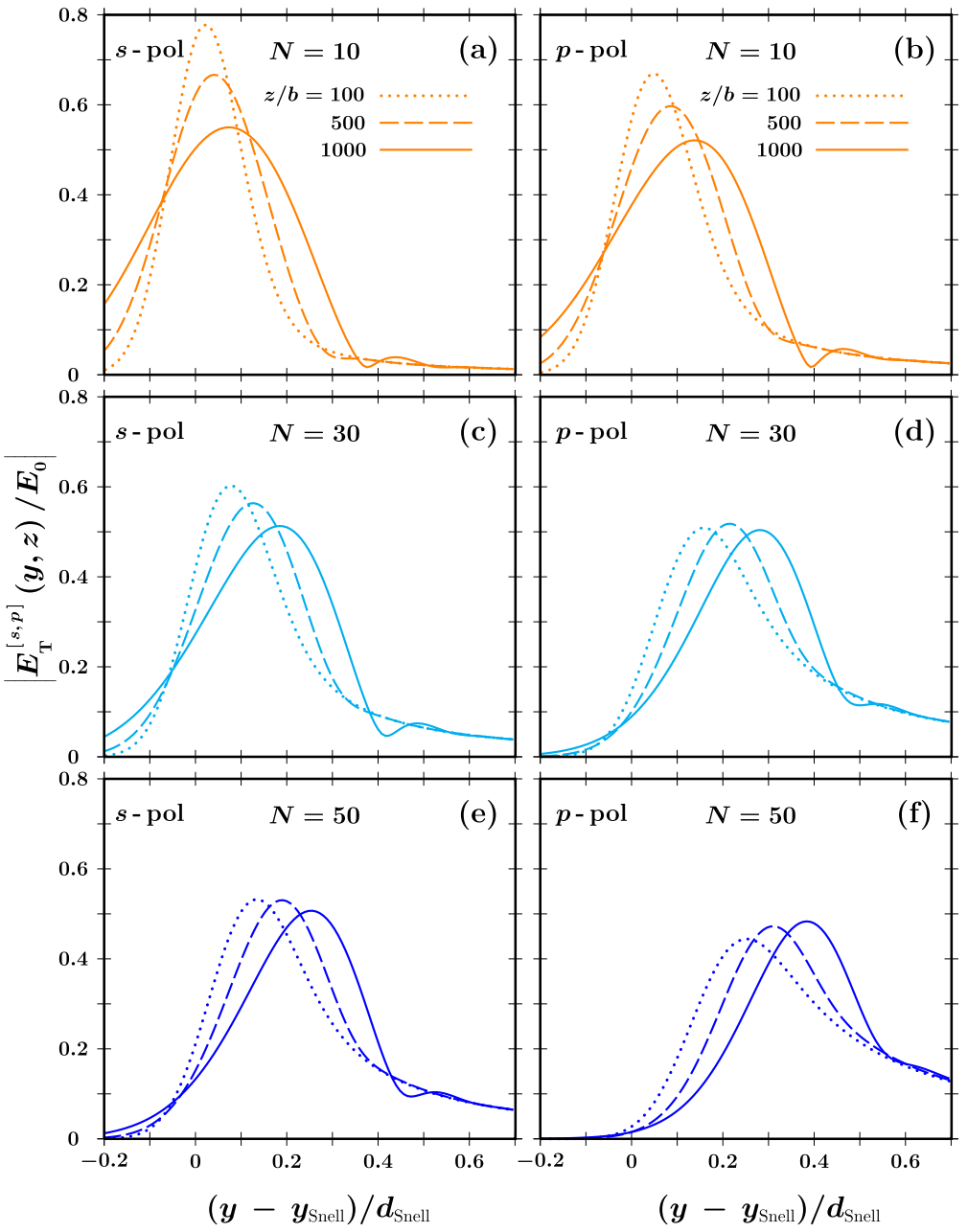

FIG. 6. (Color online) Focal effect. For $kw_0 = 10^4$, $b/w_0 = 10$ and for incidence at the critical angle, the multiple-peak phenomenon is no longer so evident. Nevertheless, a new interesting phenomenon appears. Due to the second-order optical phase contribution, in the outgoing beam a focalization effect can be now observed. This effect is clear in (f).

V. CONCLUSIONS AND OUTLOOK

The connection between quantum mechanics and optics [12] and the possibility to realize optical experiments to reproduce quantum effects [13] make optics an interesting subject of study to investigate the most diversified phenomena, from the Goos-Hänchen and Imbert-Federov shifts to the frustrated total internal reflection [33–36] and resonant photon tunneling [37]. In this paper, starting from a modeled symmetry breaking (Sec. II), we have shown *how* to reproduce the *maximal* breaking of symmetry in the angular distribution of laser beams using an optical structure composed of N dielectric blocks. This structure can be realized in a real optical experiment by a single elongated prism. The breaking of symmetry causes an *angular modification* of the optical path predicted by the Snell law. The outgoing beam is no longer parallel to the incoming one as expected from the Snell law. Our analysis shows that the maximal angular deviation is obtained for a Gaussian He-Ne laser with $\lambda = 633$ nm and beam waist $w_0 = 100\mu$m by using p-polarized waves and a dielectric structure with 50 blocks [see Fig. 2(c)]. In this case, we should find an angular deviation

$$\alpha_{\max} = \arctan\left[\frac{\int d\theta(\theta-\theta_c)f^2(\theta-\theta_c)}{\int d\theta f^2(\theta-\theta_c)}\right] = \arctan\left[\frac{\sqrt{2/\pi}}{kw_0}\right] \approx \frac{\sqrt{2/\pi}}{kw_0} \approx 0.05^\circ \frac{\pi}{180^\circ}, \quad (29)$$

TABLE II. Focal effect for BK7 and fused silica dielectric blocks. The numerical maximum of the outgoing electrical field at the critical angle $\theta_0 = \theta_c$ is listed for p-polarized waves for different refractive indexes as a function of the axial parameter z and for fixed beam waist/wavelength ratio, $kw_0 = 10^4$, and block number, $N = 50$. We clearly see the focalization near $z = 10^3 d_{\text{Snell}}$.

	$\left\|E_T^{[p]}(y, z; \theta_0)/E_0\right\|_{\max}$					
n \ z/d_{Snell}	100	500	1000	1500	2000	
$\sqrt{2}$	0.444	0.472	0.483	0.475	0.460	p-pol
1.457	0.440	0.468	0.480	0.472	0.457	
1.515	0.434	0.463	0.475	0.469	0.454	

which does not depend on the refractive index n of the dielectric blocks and does not change if we increase the block number because we have reached the maximal breaking of symmetry for $N = 50$. This prediction can be tested in real optical experiments by using different dielectric blocks, for example, fused silica and BK7 (see Table I). Nevertheless, the previous formula does *not* take into account cumulative dissipations and imperfections in the prism such as misalignment of its surfaces. A phenomenological way to include the misalignment effect in the angular deviation is to consider the following distribution:

$$f_{\text{mis}}(\theta - \theta_c) = \begin{cases} 0 & \theta - \theta_c < \theta_{\text{mis}}, \\ \exp[-(kw_0\theta)^2/4] & \theta - \theta_c \geqslant \theta_{\text{mis}}, \end{cases} \quad (30)$$

where the angle $\theta_{\text{mis}} = \arcsin[n \sin(\varphi_{\text{mis}} - \frac{\pi}{4})]$ is introduced to include misalignment effects. Such effects can be simulated by observing that the surfaces misalignment can be simulated by changing the internal angle from φ_c to $\varphi_c + \varphi_{\text{mis}}$. In this case, the angular deviation is given by

$$\alpha_{\text{mis}} = \arctan\left[\frac{\int d\theta\theta f_{\text{mis}}^2(\theta - \theta_c)}{\int d\theta f_{\text{mis}}^2(\theta - \theta_c)}\right] \approx \frac{\exp[-(kw_0\theta_{\text{mis}})^2/2]}{\text{erfc}[kw_0\theta_{\text{mis}}/\sqrt{2}]}\alpha_{\max}. \quad (31)$$

The possibility to realize a *maximal* breaking of symmetry and to make a prediction of the angular deviation of the Snell law represents the main objective of our investigation. This study, which overcomes the infinity at the critical angle through the integration of Eq. (28), also allows us to find a closed-form expression for the Goos-Hänchen shift. The prediction is in excellent agreement with our numerical calculation. Finally, but not less important, two additional phenomena appear in the presence of the symmetry breaking, namely, the multiple-peak phenomenon and the focal effect. We hope that the analysis presented in this work stimulates optical experiments to confirm the angular deviation α (Fig. 4), the multiple peaks (Fig. 5), and the focalization (Fig. 6) in the outgoing beam.

In a forthcoming paper, we aim to extend the investigation of the symmetry breaking done in this work for Gaussian angular distributions by analyzing the effect of the breaking of symmetry in Hermite- and Laguerre-Gaussian optical beams [38].

ACKNOWLEDGMENTS

The authors gratefully acknowledge Capes (M.P.A.), CNPq (S.D.L.), and Fapesp (S.A.C.) for the the financial support and the referee for his comments and suggestions, in particular for drawing attention to the misalignment effect, which stimulated the discussion which led to Eq. (31).

[1] M. Born and E. Wolf, *Principles of Optics* (Cambridge University Press, Cambridge, 1999).
[2] B. E. A. Saleh and M. C. Teich, *Fundamentals of Photonics* (Wiley, Hoboken, NJ, 2007).
[3] F. Goos and H. Hänchen, Ann. Phys. (Berlin, Ger.) **436**, 333 (1947).
[4] K. Artmann, Ann. Phys. (Berlin, Ger.) **437**, 87 (1948).
[5] C. K. Carniglia and L. Mandel, J. Opt. Soc. Am. **61**, 1035 (1971).
[6] K. W. Chiu and J. J. Quinn, Am. J. Phys. **40**, 1847 (1972).
[7] M. McGuirk and C. K. Carniglia, J. Opt. Soc. Am. **67**, 103 (1977).
[8] K. Yasumoto and Y. Oishi, J. Appl. Phys. **54**, 2170 (1983).
[9] H. M. Lai, F. C. Cheng, and W. K. Tang, J. Opt. Soc. Am. A **3**, 550 (1986).
[10] C. C. Chan and T. Tamir, J. Opt. Soc. Am. A **4**, 655 (1987).
[11] F. I. Baida, D. V. Labeke, and J. M. Vigoureux, J. Opt. Soc. Am. A **17**, 858 (2000).
[12] X. Chen, J. Opt. **15**, 033001 (2013).
[13] G. Jayaswal, G. Mistura, and M. Merano, Opt. Lett. **38**, 1232 (2013).
[14] M. Araujo, S. Carvalho, and S. De Leo, J. Mod. Opt. **60**, 1772 (2014).
[15] C. Imbert, Phys. Rev. D **5**, 787 (1972).
[16] F. Pillon, H. Gilles, and S. Girard, Appl. Opt. **43**, 1863 (2004).
[17] K. Y. Bliokh, I. V. Shadrivov, and Y. S. Kivshar, Opt. Lett. **34**, 389 (2009).
[18] C. Prajapati and D. Ranganathan, J. Opt. Soc. Am. A **29**, 1377 (2012).
[19] A. Aiello, New J. Phys. **14**, 013058 (2012).
[20] K. Y. Bliokh and A. Aiello, J. Opt. **15**, 014001 (2013).
[21] H. E. Tureci and A. D. Stone, Opt. Lett. **27**, 7 (2002).
[22] H. Schomerus and M. Hentschel, Phys. Rev. Lett. **96**, 243903 (2006).
[23] W. Guo, Opt. Commun. **278**, 253 (2007).
[24] M. Merano, A. Aiello, M. P. van Exter, and J. P. Woerdman, Nat. Photon. **3**, 337 (2009).
[25] J. B. Götte, S. Shinohara, and M. Hentschel, J. Opt. **15**, 014009 (2013).
[26] M. Araujo, S. Carvalho, and S. De Leo, J. Opt. **16**, 015702 (2014).
[27] S. De Leo and P. Rotelli, Eur. Phys. J. D **61**, 481 (2011).
[28] S. A. Carvalho and S. De Leo, J. Mod. Opt. **60**, 437 (2013).
[29] S. A. Carvalho and S. De Leo, Eur. Phys. J. D **67**, 168 (2013).
[30] E. Wigner, Phys. Rev. **98**, 145 (1955).

[31] R. B. Dingle, *Asymptotic Expansions: Their Derivation and Interpretation* (Academic, London, 1973).
[32] N. Bleistein and R. Handelsman, *Asymptotic Expansions of Integrals* (Dover, New York, 1975).
[33] S. Zhu, A. W. Yu, D. Hawley, and R. Roy, Am. J. Phys. **54**, 601 (1986).
[34] A. A. Stahlhofen, Phys. Rev. A **62**, 012112 (2000).
[35] F. P. Zanella, D. V. Magalhaes, M. M. Oliveira, R. F. Bianchi, L. Misoguti, and C. R. Mendonca, Am. J. Phys. **71**, 494 (2003).
[36] H. G. Winful and C. Zhang, Phys. Rev. A **79**, 023826 (2009).
[37] S. De Leo and P. Rotelli, Eur. Phys. J. D **65**, 563 (2011).
[38] J. Enderlein and F. Pampaloni, J. Opt. Soc. Am. A **21**, 1553 (2004).